A three-dimensional self-supporting low loss microwave lens with a negative refractive index

Citation: Ehrenberg, Isaac M., Sanjay E. Sarma, and Bae-Ian Wu. "A Three-Dimensional Self-Supporting Low Loss Microwave Lens with a Negative Refractive Index." Journal of Applied Physics 112, no. 7 (2012): 073114. © 2012 American Institute of Physics.

As Published: http://dx.doi.org/10.1063/1.4757577

Publisher: American Institute of Physics

Persistent URL: http://hdl.handle.net/1721.1/87638

Version: Final published version: final published article, as it appeared in a journal, conference proceedings, or other formally published context

A three-dimensional self-supporting low loss microwave lens with a negative refractive index

Isaac M. Ehrenberg, Sanjay E. Sarma, and Bae-Ian Wu

Citation: Journal of Applied Physics **112**, 073114 (2012); doi: 10.1063/1.4757577
View online: http://dx.doi.org/10.1063/1.4757577
View Table of Contents: http://scitation.aip.org/content/aip/journal/jap/112/7?ver=pdfcov
Published by the AIP Publishing

A three-dimensional self-supporting low loss microwave lens with a negative refractive index

Isaac M. Ehrenberg,[1] Sanjay E. Sarma,[1] and Bae-Ian Wu[2]
[1]*Auto-ID Labs, Massachusetts Institute of Technology, Cambridge, Massachusetts 02139, USA*
[2]*Sensors Directorate, Air Force Research Laboratory, Wright Patterson AFB, Ohio 45433, USA*

(Received 5 July 2012; accepted 5 September 2012; published online 11 October 2012)

Demonstrations of focusing with metamaterial lenses have predominantly featured two dimensional structures or stacks of planar elements, both limited by losses which hinder realized gain near the focal region. In this study, we present a plano-concave lens built from a 3D self-supporting metamaterial structure featuring a negative refractive index between 10 and 12 GHz. Fabricated using macroscopic layered prototyping, the lens curvature, negative index and low loss contribute to a recognizable focus and free space gains above 13 dB. © *2012 American Institute of Physics*. [http://dx.doi.org/10.1063/1.4757577]

I. INTRODUCTION

The development of metamaterials has accelerated over the last decade in efforts to understand the feasibility of tuning electromagnetic material properties toward useful applications. Starting from arrays of holes, pillars, and planar metallic structures[1] at microwave frequencies, previously unobserved but understood[2] physical phenomena have since been demonstrated beyond the optical regime including negative permeability, permittivity, and refractive index.[3] These innovations led to the development of theory and experiments which promised futuristic technologies such as invisibility cloaks,[4–6] and perfect lenses[7–9] capable of imaging point sources beyond the diffraction limit.

Despite significant progress, practical challenges remain when it comes to metamaterial fabrication and reducing material losses within devices. The early success and evolution of metamaterials were due in part to the availability of robust planar fabrication techniques including printed circuit boards and silicon based microfabrication. As a result, realizations have predominantly featured two-dimensional (2D) arrays of planar structures limited dimensionally and hindered by material losses. Dispersive combinations of conductors and dielectrics coupled with resonances result in unwanted reflections and dissipation that diminish performance.[10] Loss is especially pronounced in three dimensional metamaterials, which consist of stacked or weaved lattices of 2D arrays.[11,12] Each layer absorbs a percentage of the transmitted energy, severely reducing the output of multilayer devices.

Several metamaterial unit cell designs with self-supporting three-dimensional (3D) geometries have been proposed that aim to reduce losses by eliminating the use of dielectric substrates.[13–16] While these structures are more complex making fabrication difficult, we are now able to realize them by taking advantage of advances in macroscopic layered prototyping, through technologies such as stereolithography, selective laser sintering, fused deposition modeling, and three-dimensional printing. Once limited to flimsy prototypes, these methods are now used to produce functional parts including advanced electromagnetic components. For example, layered prototyping was recently employed in the assembly of an alumina gradient index lens,[17] 3D split ring resonator (SRR) array,[18] volumetric perfect lens,[19] and Luneburg antenna.[20]

In this work, we combine the flexibility of macroscopic layered prototyping and advantages of self-supporting unit cells to fabricate a low-loss 3D metamaterial. To exemplify its utility, we construct a plano-concave lens for microwave frequencies featuring a negative refractive index (NRI). The low-loss behavior of the material is verified experimentally, while the performance of the assembled lens matches that predicted by simulations, with the measured focal field enhancements higher than previously reported for similar lenses.

II. NEGATIVE INDEX LENS

Imaging and focusing are two of the primary uses for lens technology and are seen as possible venues for metamaterial enhancement. Much attention has been given to the perfect lens, which requires cuboid or cylindrical geometries and a refractive index of -1 to enable sub-diffraction imaging of objects nearby. The focusing of incident plane waves with homogeneous material is not possible without lenses sporting more complex geometric profiles.[2] Lenses made from positive index material with spherical or hyperbolic curvatures can focus incident plane waves, but reflections and aberrations limit transmitted intensity and increase the size of the focal region. Plano-concave lenses of negative index material allow for such focusing with fewer reflections and decreased aberrations, which can result in a tighter focus with increased intensity.[21] Additionally, NRI materials often have a lower density than conventional positive index materials, resulting in lighter weight systems.[22]

Past implementations of NRI plano-concave lenses have relied on arrays of SRRs and wires to obtain the required negative constitutive parameters.[23] Focusing is observed, but material losses compounded through the multilayer structures prevent significant intensity gains when compared to an open aperture, reaching only as high as 5 dB. Alternative plano-concave lens constructions which avoid the complexities of 3D SRR assemblies, such as arrays of holes milled

into thin metal sheets, also fail to produce significant gains in the focal region.[24]

In our implementation, we used a modified S-ring metamaterial cell similar to Moser *et al.*,[25] as shown in Fig. 1, to realize an NRI for the plano-concave lens. We modeled wave propagation through the structure and simulated the scattering parameters using commercial finite element software (HFSS, Ansoft). We retrieved effective material parameters following a standard procedure outlined by Chen *et al.*[26] Though the imaginary part of the derived permittivity is negative below 10 GHz precluding the classification of this structure as an effective medium in that regime,[25] simultaneous negative permeability and permittivity between 10 and 12 GHz result in a low-loss NRI region with values ranging from −2 to 0 (Fig. 2).

We designed the NRI lens by virtually stacking seven S-ring arrays atop one another, with 1.5 mm between each layer. Unit cells were removed from the top six layers to give the stack a discretized concave curvature approximating a hyperbolic surface $S(r)$ where

$$(f - n \cdot r)^2 = (S(r))^2 + (f - r)^2, \tag{1}$$

in which $r^2 = x^2 + z^2$ such that plane waves incident upon the planar surface of an ideal planoconcave lens with this profile focus at a distance $f = 90$ mm, given a refractive index of $n = -1$.

We fabricated polymer S-ring arrays using commercial layered prototyping equipment (Connex 500, Objet). After removal of the support material with the aid of a 2% NaOH bath and high pressure water jet system, a sputtering process coated each layer with 4 μm of copper. We limited both the time and rate of the copper deposition in order to minimize warping of the polymer matrix due the extreme temperatures that result from the lack of heat transfer through the vacuum of the sputtering chamber. Although sputtering is a directional process, the open cellular architecture of the S-ring array allowed for sufficient coating of sidewall surfaces. While the underlying polymer base is required for structural support, the conformal coverage and thickness of the copper layer, well above the 0.64 μm skin depth at 10 GHz, minimize loss due to interactions between the dielectric and incident electromagnetic wave. To ease final assembly, solid blocks featuring predefined holes were included at the corners of each layer, through which nylon bolts were inserted. Plastic washers and foam were used to separate the layers. The weight of the assembled lens was 420 grams.

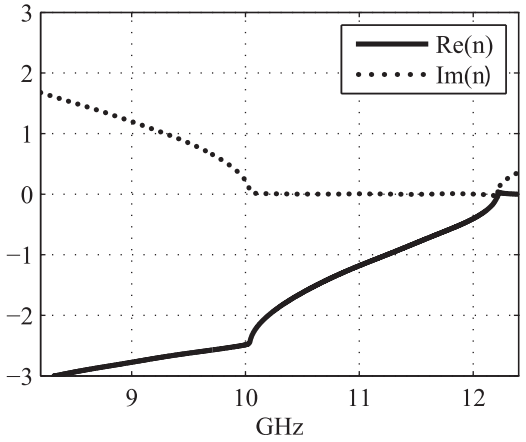

FIG. 2. Real and imaginary parts of the S-ring's retrieved refractive index. The imaginary part is near zero between 10 and 12 GHz, while the real part is negative.

III. RESULTS

To experimentally verify the low loss behavior of the S-ring structure, the transmissivity of one complete layer was measured (Fig. 3). The layer, oriented as in Fig. 1(a) with respect to the incident signal, was placed between two horn antennas spaced just over 4.5 mm apart. Though a small portion of the signal escapes due to the finite horn aperture, causing a 2 dB drop in received power across all frequencies, the fact that the peak S21 of the signal transmitted through the metamaterial layer reaches the same level as transmission between the horns through just air confirms the expected loss characteristics. The observed pass band also coincides with the negative refractive index region predicted by simulations. Lower transmission levels at frequencies above the transmission peak are attributed to reflections caused by the impedance mismatch with free space, as opposed to absorption within the metamaterial.

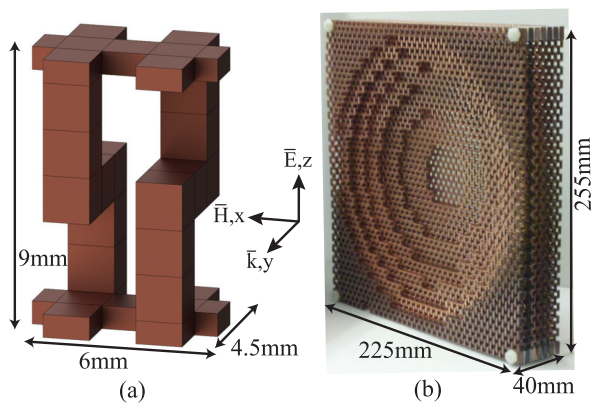

FIG. 1. (a) Solid model of the S-ring unit cell, the response of which is polarization dependent, and (b) a photograph of the assembled planoconcave lens which consists of 7 metamaterial layers in the propagating direction.

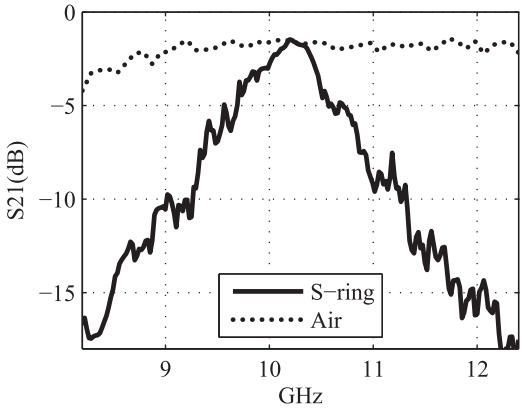

FIG. 3. The measured transmission through one copper clad S-ring array layer compared to transmission through air. S21 for the copper samples reaches the level of air near 10.25 GHz.

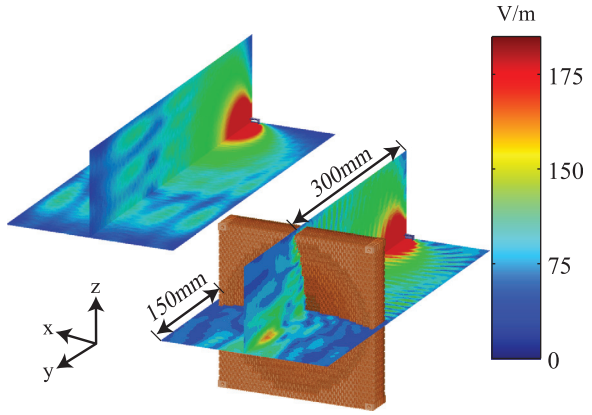

FIG. 4. Simulated E-Field magnitude with and without the lens at 10.9 GHz.

The setup used to evaluate the lens experimentally consisted of the lens centered on the y-axis occupying the space between $y = -40$ mm and 0 mm, and a transmitting antenna placed at $y = -340$ mm facing the planar surface of the lens. The distance between the transmitter and lens was 300 mm, ten times the wavelength at 10 GHz, enough for the signal incident on the lens to resemble a plane wave. A receiving X-band horn antenna was placed on a computer controlled XYZ stage directly behind the concave side of the lens. The antenna was stepped at 7.5 mm intervals throughout a $(150\,\text{mm})^3$ volume and the received power was recorded for 200 frequencies from 8.2 to 12.4 GHz to build a 3D spatial power map. The Z-stage holding the receiver consisted of nonmetal parts to minimize spurious reflections that could disturb the measurements.

Numerical simulations of the experimental setup were performed with and without the lens in place. The results show that while the E-field disperses and weakens as waves propagate away from the small aperture source, we observe focusing in the presence of the lens with the E-field magnitude in the focal region much greater than without the lens (Fig. 4).

Physical measurements were also taken both with and without the lens in place. A plot of the measured received power levels at 10.9 GHz in the XY and YZ planes behind the lens (Fig. 5) clearly shows focusing of the power to a

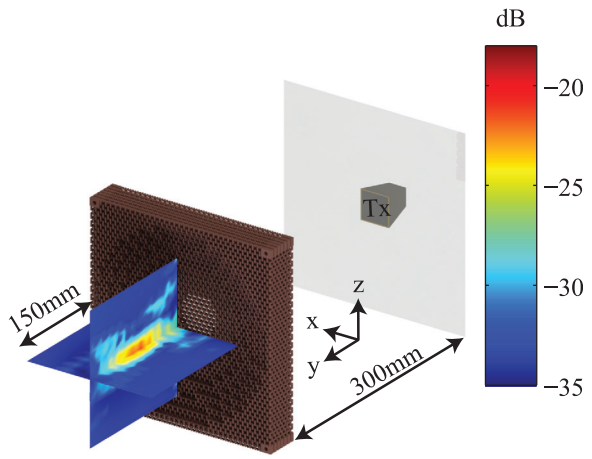

FIG. 5. The experimental setup and plot of experimentally measured power received though the lens at 10.9 GHz, including the focal region approximately 75 mm behind the lens.

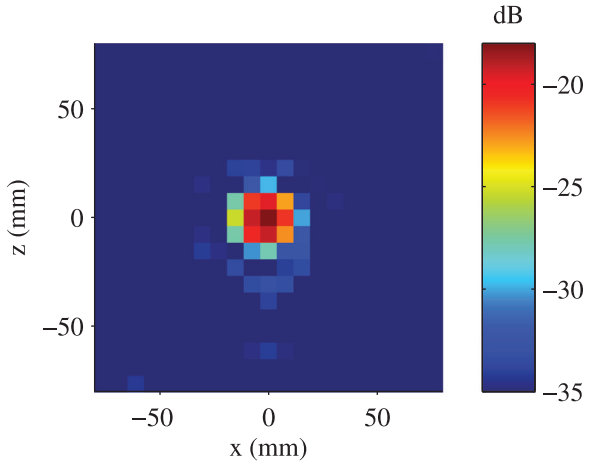

FIG. 6. The received power measured on the focal plane y = 75 mm at 10.9 GHz.

small region centered at 75 mm from the back of the lens. The measurements in the XZ plane at $y = 75$ mm for the same frequency show both a neat focal area and power levels reaching −18 dB (Fig. 6). When compared to power levels below −30 dB without the lens in place, the focal gain reported here is much higher than previous metamaterial lenses. We attribute this high gain to both the enhanced intensity expected for NRI plano-concave lenses, and the inherent low loss of the self-supporting metamaterial design. The focal region appears to have a 3 dB spot width in the X and Z directions of less than 7.5 mm. That estimate is limited by the measurement aperture and step size and could become significantly smaller with more dense sampling in the focal region, which was not performed in this study due to time constraints. While the focal region is centered on the Y-axis as expected, asymmetry in the focal fields is apparent from the measurements, presumably due to reflections from the environment and tolerances in the test setup and fabrication.

While the highest received power measured in this experiment was at 10.9 GHz, the focusing effect and gain of the lens was not limited to a single frequency but evident throughout the entire NRI band of the S-ring (Fig. 7), where heightened intensity levels were recorded. A mapping of the

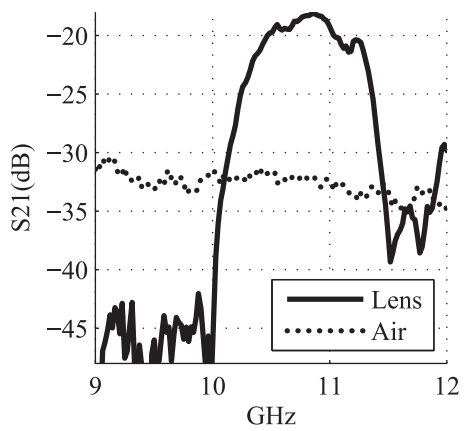

FIG. 7. The measured received power at y = 75 mm on the y-axis with the lens in place is much higher than without the lens within a large swath of the NRI band of the S-ring.

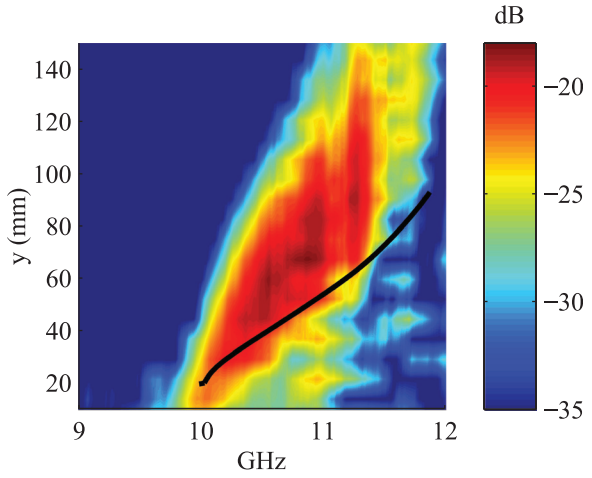

FIG. 8. The measured power along the y-axis. The line represents the calculated focal length of a theoretical thin lens with the same plano-concave curvature and frequency dependent refractive index.

measurements along the y-axis shows there are distinct focal regions at each frequency (Fig. 8). These areas of high intensity move away from the lens as the frequency rises. This is due to the frequency dependent refractive index of the S-ring unit cell. The trend correlates well with the expected chromatic shift in focal distance of a homogeneous lens of similar geometry and material properties. Below 10 GHz, there is no focusing despite the negative refractive index because the imaginary part is too high. The lens approximation seems to break down as the frequency approaches 12 GHz, where the refractive index is a very small negative number, corresponding to the region of extraordinary transmission. Though the focal position measurements match fairly well with the calculations based on the refractive index retrieved from simulations, slight deviations of the measured results are caused by a number of factors including the metamaterial layer discretization, and variations in the distance between individual layers of the assembled lens. Bowing or bending of the layers away from one another changes the overall unit cell thickness which can raise the refractive index at each frequency in the NRI band, moving the focus further away from the lens or vice versa.

IV. CONCLUSION

In this paper, we report on the design, rapid fabrication, and evaluation of a planoconcave lens featuring a negative refractive index assembled from self-supporting metamaterials. The 255 mm × 225 mm × 40 mm freestanding lens operates within the 10–12 GHz band, with a frequency dependent focal length ranging of 6–10 cm. The low loss, high gain performance of this lightweight lens predicted by simulation and corroborated by experiment demonstrates the ability to construct NRI devices with quality material parameters. The fabrication flexibility afforded by rapid prototyping technology suggests that complex unit geometries and devices consisting thereof are readily accessible, which promise to further the actualization of metamaterial performance benefits.

[1]J. Pendry, A. Holden, D. Robbins, and W. Stewart, Microwave Theory Tech. **47**, 2075 (1999).
[2]V. G. Veselago, Phys. Usp. **10**, 509 (1968).
[3]V. M. Shalaev, Nature Photon. **1**, 1749 (2007).
[4]J. Pendry, D. Schurig, and D. Smith, Science **312**, 1780 (2006).
[5]D. Schurig, J. Mock, B. Justice, S. Cummer, J. Pendry, A. Starr, and D. Smith, Science **314**, 977 (2006).
[6]R. Liu, C. Ji, J. Mock, J. Chin, T. Cui, and D. Smith, Science **323**, 366 (2009).
[7]J. B. Pendry, Phys. Rev. Lett. **85**, 3966 (2000).
[8]N. Fang, H. Lee, C. Sun, and X. Zhang, Science **308**, 534 (2005).
[9]Z. Lu, J. Murakowski, C. Schuetz, S. Shi, G. Schneider, and D. W. Prather, Phys. Rev. Lett. **95**, 153901 (2005).
[10]M. W. C. M. Soukoulis and S. Linden, Nature Photon. **5**, 523 (2011).
[11]C. Soukoulis, S. Linden, and M. Wegener, Science **315**, 47 (2007).
[12]N. I. Zheludev, Science **328**, 582 (2010).
[13]B. Burckel, J. Wendt, G. Eyck, R. Ellis, I. Brener, and M. Sinclair, Adv. Mater. **22**, 3171 (2010).
[14]D. Gney, T. Koschny, M. Kafesaki, and C. Soukoulis, Opt. Lett. **34**, 506 (2009).
[15]D. Gney, T. Koschny, M. Kafesaki, and C. Soukoulis, Opt. Express **18**, 12348 (2010).
[16]M. W. C. M. Soukoulis, Science **330**, 1633 (2010).
[17]H. Wang, M. Cima, B. Kernan, and E. Sachs, J. Non-Cryst. Solids **349**, 360 (2004).
[18]P. Mercure, P. Haley, A. Bogle, L. Kempel, in *Antennas and Propagation Society International Symposium* (2005), Vol. 1B, pp. 623–626.
[19]A. G. S. Rudolph and C. Pfeiffer, IEEE Trans. Antennas Propag. **59**, 2989 (2011).
[20]M. Liang, W. Ng, K. Chang, M. Gehm, and H. Xin, in *IEEE Microwave Symposium Digest* (IEEE MTT-S International, Baltimore, MD, 2011), pp. 1.
[21]D. S. D. Schurig, Phys. Rev. E **70**, 065601 (2004).
[22]C. Parazzoli, R. Greegor, J. Nielsen, M. Thompson, K. Li, A. Vetter, M. Tanielian, and D. Vier, Appl. Phys. Lett. **84**, 3232 (2004).
[23]R. Greegor, C. Parazzoli, J. Nielsen, M. Thompson, M. Tanielian, D. Vier, S. Schultz, D. Smith, and D. Schurig, IET Proc. Microwaves, Antennas Propag. **1**, 108 (2007).
[24]M. Beruete, M. Navarro-Cía, M. Sorolla, and I. Campillo, Opt. Express **16**, 9677 (2008).
[25]H. Moser, J. A. Kong, L. Jian, H. Chen, G. Liu, M. Bahou, M. Kalaiselvi, S. Maniam, X. Cheng, B. Wu *et al.*, Opt. Express **16**, 13773 (2008).
[26]X. Chen, T. M. Grzegorczyk, B.-I. Wu, J. Pacheco, and J. A. Kong, Phys. Rev. E **70**, 016608 (2004).